Available online at www.sciencedirect.com
SCIENCE DIRECT®
Journal of Hydrology 299 (2004) 166–179
Journal of Hydrology
www.elsevier.com/locate/jhydrol

Temporal and spatial resolution of rainfall measurements required for urban hydrology

Alexis Berne[a,b,*], Guy Delrieu[b], Jean-Dominique Creutin[b], Charles Obled[b]

[a]*Hydrology and Quantitative Water Management Group, Nieuwe Kanal 11, Wageningen PA6709, The Netherlands*
[b]*Laboratoire d'étude des Transferts en Hydrologie et Environnement, Grenoble, France*

Abstract

The objective of the paper is to provide recommendations on the temporal and spatial resolution of rainfall measurements required for urban hydrological applications, based on quantitative investigations of the space-time scales of urban catchments and rainfall. First the temporal rainfall–runoff dynamics is studied using lag time values derived from rainfall and discharge time series for a set of urban catchments. Then the temporal and spatial structure of rainfall is analysed with high resolution rain gauge and radar measurements from the HYDROMET Integrated Radar Experiment '98 experiment for three typical intense Mediterranean rain events. In particular the evolution of the structure of the rainfall field at different time steps is investigated using geostatistics. Finally the required space-time resolution of rainfall for Mediterranean regions is estimated as a function of the surface of the catchments. According to the results, hydrological applications for urban catchments of the order of 1000 ha require a temporal resolution of about 5 min and a spatial resolution of about 3 km. For urban catchments of the order of 100 ha, it becomes a resolution of about 3 min and 2 km, that common operational networks or radars cannot provide. These results complement the scarce recommendations on resolution of rainfall for urban hydrology reported in the literature.

Keywords: Urban hydrology; Lag time; Rainfall structure; Space-time resolution; Geostatistics

1. Introduction

The role of rainfall is essential for urban hydrology: it is the driving phenomenon of runoff mechanisms, particularly in an urban context. Its variability constitutes a significant source of uncertainty for hydrological modelling. The small size of the urban catchments and the hydrological purposes (especially for real time applications) oblige us to consider rainfall at small scales: on the order of 10 min in time and 10 km in space. Hence urban hydrology requires rainfall measurements with high temporal and spatial resolutions (Berndtsson and Niemczynowicz, 1988; Niemczynowic, 1999; Ogden et al., 2000). National or regional rain measurement networks have not such high resolutions and specific networks devoted to urban hydrology must be built.

Schilling (1991) describes and quantifies the requirements about rainfall data for urban hydrology.

* Corresponding author. Address: Hydrology and Quantitative Water Management Group, Nieuwe Kanal 11, Wageningen PA6709, The Netherlands. Tel.: +31 417 48 57 60.
E-mail address: alexis.berne@wur.nl (A. Berne).

0022-1694/$ - see front matter © 2004 Elsevier B.V. All rights reserved.
doi:10.1016/j.jhydrol.2004.08.002

The discrepancy between theoretical and actual rain measurements, mainly due to practical and financial reasons, is underlined. The author gives numerical recommendations to design rain gauge networks for different hydrological applications like the design, the evaluation or the real time control of a drainage network. However, because of the lack of quantitative investigations, these numbers are 'guesstimates' according to the author.

One of the objectives of HYDROMET Integrated Radar Experiment '98 (HIRE'98) (Uijlenhoet et al., 1999) was to obtain improved rainfall measurements, above a large urban area. During the experiment, an important data set of high resolution rainfall measurements from different sensors (rain gauge, radar, disdrometer for example) was collected. A 'historical' archive of discharge measurements for several urbanised catchments was also available. This data set offers the opportunity to quantify the temporal and spatial scales of different urban catchments (the hydrological systems to characterise) and those of rainfall (the main input into the systems).

The purpose of the paper is to give a quantitative basis to the requirements about temporal and spatial resolutions for rainfall measurements dedicated to urban hydrology, using a high resolution precipitation data set. The studied area and the HIRE'98 experiment are presented in Section 2. In Section 3, we investigate the temporal and the spatial scales of different urban catchments by analysing rainfall and discharge time series. Using geostatistics, the temporal and spatial structures of rainfall are studied in Section 4, with a highlight on the effect of time averaging. Based on the results of Sections 3 and 4, the temporal and spatial resolution of rain measurement relevant for urban hydrology can be finally assessed in Section 5. The adequacy of some operational networks is analysed from this point of view.

2. Data set

2.1. Marseille area

This paper is based on data collected in the town of Marseille, south-east of the French Mediterranean coast. Marseille is a large city of about 800.000 inhabitants, which covers a surface of 240 km^2 and is surrounded by low level mountains (Fig. 1). Because of the Mediterranean climate, precipitation can be very violent (especially in autumn). A city service has

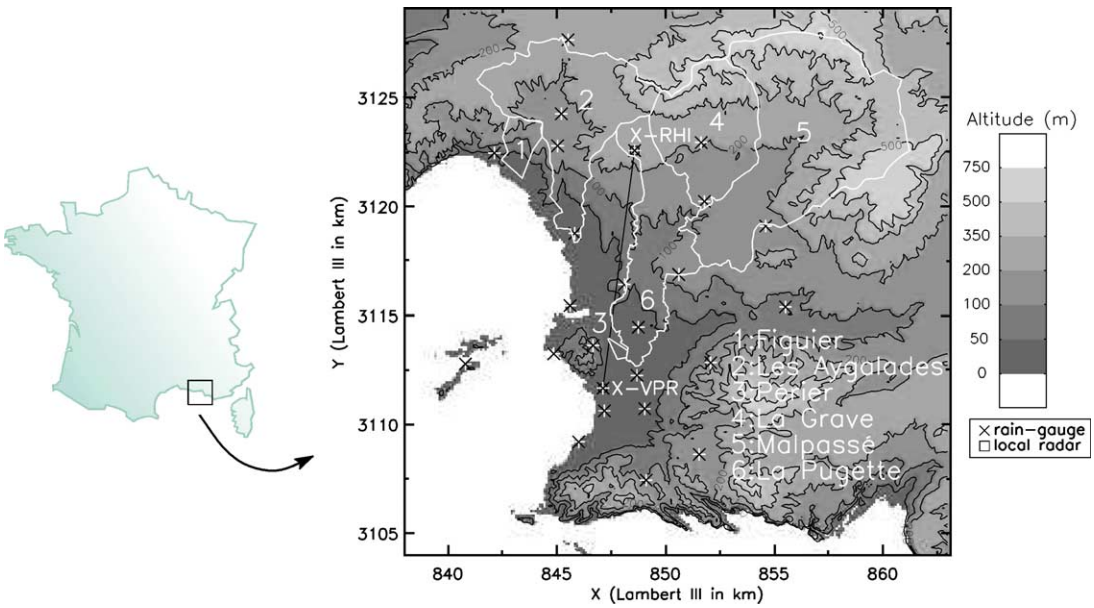

Fig. 1. Marseille area and location of the different sensors. Contours of the six studied catchments are drawn in white.

been created to manage the sewage system and to limit hazards due to flash floods. Different monitoring systems have been deployed, in particular (i) a telemetering tipping-bucket rain gauge network (25 gauges, spatial density about 1 gauge per 12 km^2, 6 min time step) and (ii) a telemetering stage network (about 100 gauges, 6 min time step) more specifically devoted to monitor the sewage system. These sensor networks are maintained and checked regularly, providing reliable data. Rain gauge and stage measurements are archived since 1987. Moreover storm reports are elaborated after every rain events which required interventions from the city service. These reports constitute a data base of intense events.

Thanks to the information given by the group in charge of the maintenance of the networks, it has been possible to select six stage recorders in which height measurements can be reliably converted into discharge values. Hence we can define six catchments associated to the six recorders (see Fig. 1). A wide range of surface and imperviousness is covered by the set of catchments considered (Table 1). Surface comes from 38 ha (Périer) to 105 km^2 for La Pugette. Imperviousness comes from 8% (Malpassé) to 60% (Périer). Slope of the main channel comes from 1% (Périer) to 10% (Figuier). The imperviousness decreases when the basins cover (partially) the surrounding mountains. We can notice that there are three nested basins: La Grave, Malpassé and La Pugette. They correspond to a small river called Le Jarret.

These networks and this set of catchments are only one part of the data used in this study. High resolution data comes from the HIRE'98 experiment.

2.2. HIRE'98 experiment

The HIRE'98 took place in Marseille during the autumn 1998 (Uijlenhoet et al., 1999). By gathering different sensors at the same place, HIRE'98 was aimed to study intense Mediterranean precipitation and their hydrological impacts over a large urban area. In this study we have specifically used the following measurement devices (see Fig. 1 for location):

- An X-band weather vertically pointing radar (X-VPR hereafter) located downtown and managed by the Water Management Research Centre (WMRC), University of Bristol, United Kingdom. The height time indicator (HTI) produced have a temporal resolution of 4 s and a spatial one of 7.5 m. The 3 dB radar beam width is 1.8°.
- An X-band weather radar performing vertical plan cuts of the atmosphere (called range height indicator, hence the name of X-RHI for this radar hereafter) located in the suburbs and managed by the Laboratoire d'étude des Transferts en Hydrologie et Environnement (LTHE), Grenoble, France. The time step is 1 min. The radial resolution is 250 m and the 3 dB radar beam width is 1.8°. The polar measurements have been projected into a Cartesian grid of 250 m in the horizontal and 125 m in the vertical. X-RHI was implemented in order to contain the X-VPR beam in its scanning vertical plane (see Fig. 2).

These two radars provide high temporal and spatial resolution measurements and offer the opportunity to study rainfall at very small scales.

Table 1
Characteristics of the six selected catchments

Name	Size (ha)	Imperviousness (%)	Slope (%)	Length (m)	Lag time in min (numbers of events)
Figuier	291	29	9.3	2990	11.5 (2)
Le Aygalades	2840	18	6.7	16,245	35 (4)
Périer	38	60	1.3	1205	13.5 (4)
La Grave	2357	9	7.7	8875	30 (4)
Malpassé	8219	8	7.5	16,030	43 (5)
La Pugette	10,494	17	6.6	24,080	57 (2)

The mean lag time is given, with the number of events on which it is calculated between parenthesis. The method to estimate the lag time is presented in Section 3.

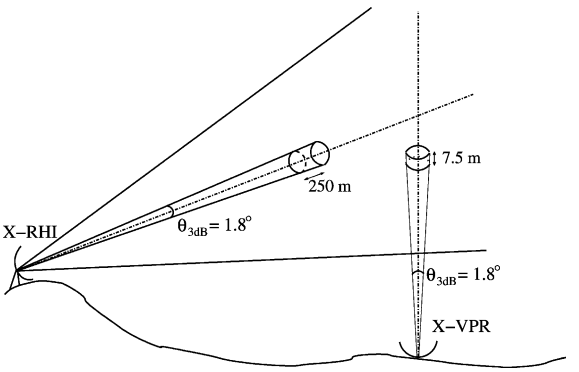

Fig. 2. Relative configuration of the two local X-band radar systems.

2.3. Radar rainfall measurement

In order to combine all the available rainfall measurements collected during the experiment in a rigorous way, it is first necessary to explain the radar rain measurement.

A radar measurement corresponds to a significant resolution volume in space. It can be assimilated to a truncated cone, which is defined by the sampling characteristics of the radar. The length is given by the radial resolution (7.5 m for X-VPR and 250 m for X-RHI), which is constant. The diameter depends on the radar beam width (1.8° for both radars) and on the distance from the radar. It is about 3 m at a distance of 100 m from the radar and about 300 m at a distance of 10 km. Hence the radar is a range dependent resolution sensor.

The temporal resolution of a radar measurement is more complex to define. The measure itself is quasi-instantaneous and it is repeated with a given time period (4 s for X-VPR and 1 min for X-RHI). But the temporal representativeness at ground level of a radar measurement (relevant for comparison with rain gauge measurements) is linked to the transit time of the rain drops in the resolution volume. Considering a mean fall velocity of about 4 m s^{-1}, the transit time is about 2 s for X-VPR at an altitude of 100 m and about 40 s for X-RHI at a distance of 10 km from the radar and for a low elevation angle.

In the following, we shall assume (i) the X-VPR measurements to be representative of the whole 4 s time step and (ii) the X-RHI measurements in the Cartesian grids to be representative of the whole 1 min time step. We must keep in mind the Cartesian resolution is not the actual radar resolution.

Studying intense rainfall with X-band radar systems, the main source of error comes from the attenuation of the radar signal by precipitation. An extensive work has been done on the co-calibration of the two radars and on the attenuation correction (Berne et al., submitted), in order to obtain reliable rain measurements.

As a remote sensor, a radar does not directly measure the rain intensity but a related variable called reflectivity. The reflectivity Z is converted in rain intensity R using the following Z–R relation: $Z = 236R^{1.53}$, where Z is expressed in $mm^6\ m^{-3}$ and R in $mm\ h^{-1}$. It has been derived from local measurements of the drop size distribution (DSD) during previous work at the same place and for similar rain events (Delrieu et al., 1997).

2.4. Selected rain events

Among all the rain events registered during the HIRE'98 experiment, we have selected the three most intense ones in terms of rainfall intensity and total rain amount: they occurred on the 7th, 11th September and 5th October 1998. Fig. 3 presents the maps of the total rain amounts for the three rain events. These maps have been obtained by interpolating the rain gauge network measurements using the kriging technique. Table 2 gives characteristic figures in terms of duration, total rain amount and maximal rain intensity recorded. The 7th September event is a very intense rain event with total amount in 5 h above 40 mm all over the area. The maximum intensity peak recorded was about 150 mm h^{-1} (in 6 min). The 11 September event is less violent with total amount in 3 h between 20 and 40 mm. The maximum intensity peak is about 60 mm h^{-1} (in 6 min). The 5th October event presents very variable amounts: some gauges did not record any rainfall (in the north of the area) while one other gauge recorded a total amount of 60 mm (in the south-west of the area). The maximum intensity peak is about 40 mm h^{-1} (in 6 min). These three rain events are representative of the Mediterranean precipitation.

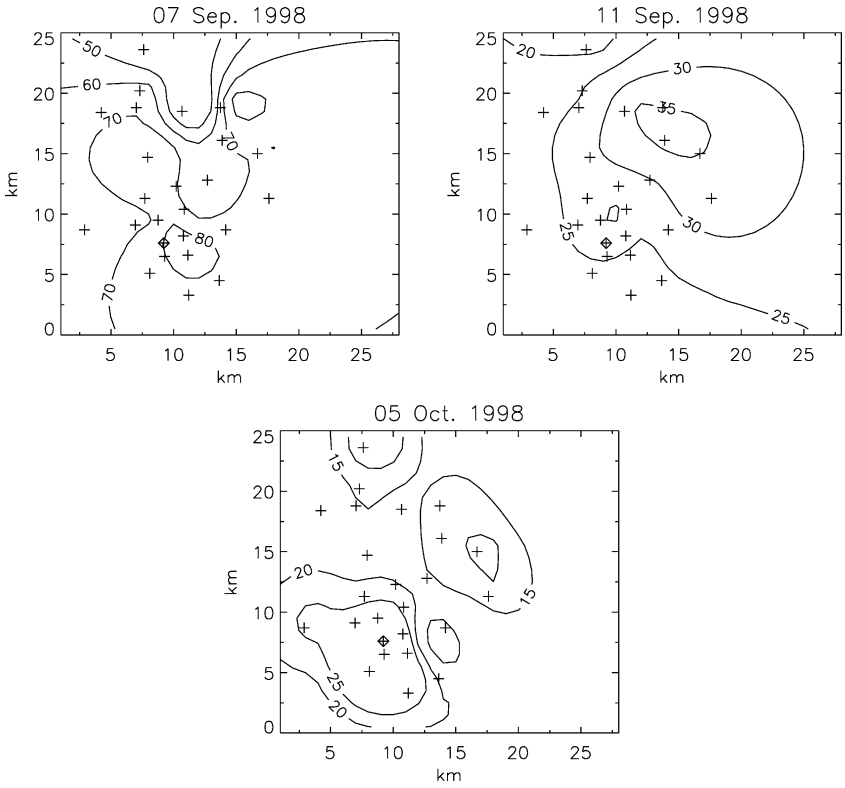

Fig. 3. Total rain amount (in mm) for the three rain events.

3. Temporal and spatial scales of urban catchments

A catchment can be seen as a low pass filter which integrates a main input (rainfall) and produces a time series output (discharge). The characteristic time associated to such a filter defines its temporal dynamics. This temporal scale determines the minimum time resolution needed for the input signal to avoid smoothing the filter response

$$\Delta t = \frac{t_c}{4} \tag{1}$$

where Δt is the time resolution and t_c, the characteristic time of the system. The factor 4 is an order of magnitude and it depends on the catchment studied and the wished accuracy (Schilling, 1991).

The characteristic time of a catchment can be assessed using its response to a pulse input of rainfall. Ideally, this characteristic time should be the time to peak of the unit-pulse response function. However, actual rainfall does not provide a real input pulse. So we consider a mean rainfall over a given catchment which is as close as possible to a pulse: mono-peak, short duration and high maximum rain intensity. Among the different possibilities to define the (hydrological) characteristic time of a basin (Schilling, 1991; Morin et al., 2001), we choose to use the lag time which is the time difference between the gravity centre of the mean rainfall over

Table 2
Characteristic figures of the three selected rain events

Event	Duration	Min. and max. rain amount (mm)	Max. intensity (in 6 min) (mm h^{-1})
09/07	5 h	20–85	160
09/11	3 h	16–40	60
10/05	4 h 30 min	0–60	40

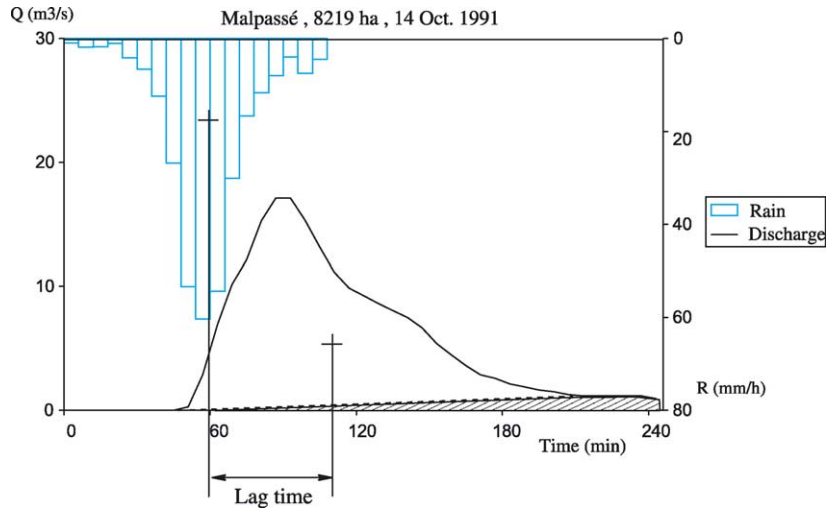

Fig. 4. Example of rainfall and discharge for the Malpassé basin during the 14 October 1991 event. The hashed part of the hydrograph corresponds to the slow component, not taken into account for the lag time calculation.

the catchment on one hand and the gravity centre of the generated hydrograph on the other hand. This definition allows to consider rain inputs which are not perfect pulses.

For each of the six catchments, we have selected several rain events fulfilling these criteria (see Table 1). The corresponding mean rainfall over the basins has been calculated by kriging the rain gauge measurements. The stage measurements have been converted into discharge measurements using for every recorder rating curves provided by the service in charge of the sensors. For catchments which have a significant rural part, the discharge response can present a 'slow' component due to the discharge contribution from the rural areas. But we are interested in the temporal dynamics of the fast component of discharge. A basic technique was applied to separate fast and slow components of hydrographs: assuming the falling limb follows two different exponential laws for the fast and slow contributions, we searched for a break in the falling limb of the hydrograph in a logarithmic scale. The centre of gravity of the hydrograph was then calculated only for the fast component (see Fig. 4).

The obtained values of characteristic time are displayed in Fig. 5. The mean lag times for each

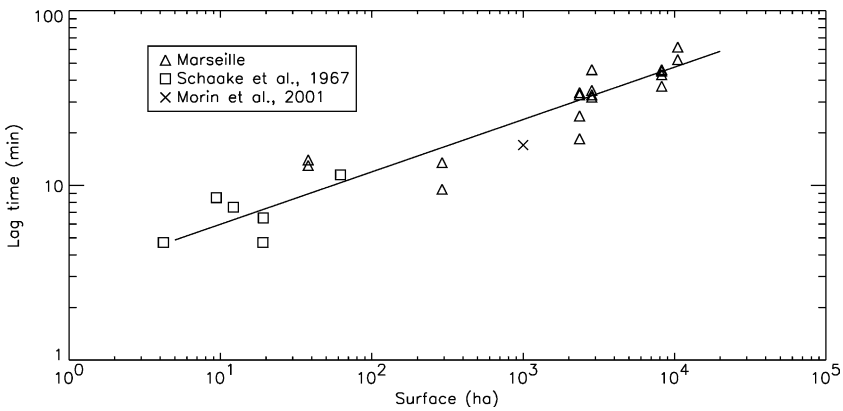

Fig. 5. Lag time (in min) versus surface (in ha), for the selected catchments. Values from Schaake et al. (1967) and Morin et al. (2001) have been added. The chosen model ($t=3S^{0.3}$) is drawn in solid line.

catchment are listed in Table 1. Values from Schaake et al. (1967) and Morin et al. (2001), obtained for catchments with similar geomorphological characteristics, have been added to assess the reliability of our values and to increase the size of the catchment sample. We must notice that (i) the sample of rain events is limited for each basin (between 2 and 5, see Table 1) and (ii) the temporal resolution of the rain gauge and stage network is probably too coarse to correctly describe the dynamic of the smallest basins (Périer and Figuier). However, we consider the estimated values provide a reliable order of magnitude of the lag time because of the limited dispersion of the values. Moreover, they are consistent with literature values.

The reduced dispersion of the scatterplot in Fig. 5 (correlation coefficient of 0.96) suggests a power law relation between the lag time and the surface of a catchment. To assess the consistency of such a relation, a multiple regression analysis is performed on the logarithmic values of the geomorphological data from our sample of catchments including data from Schaake et al. (1967) (Morin et al., 2001 do not give the imperviousness in their article). Because of the high correlation (about 0.99 for the logarithmic values) between the surface and the length, we reduce the number of independent variables and work only with the logarithms of the surface, the imperviousness and the slope. The surface appears as the most significant variable for the lag time with a partial correlation coefficient of about 0.94. It is about 0.74 for the slope and 0.007 for the imperviousness. Consequently a power law relation between the surface and the lag time is relevant. Obviously other parameters impact the characteristic time of a catchment. But in a first approximation, it mainly depends on the surface of the basin, which can be seen as its spatial scale.

A simple power law relation between lag time (t_l in min) and surface (S in ha) correctly fits the scatterplot (see Fig. 5):

$$t_l = 3S^{0.3} \tag{2}$$

We have then a quantitative link between the temporal scale (given by the lag time) and the spatial scale (given by the surface) of a basin. The validity of the fitted relation is limited because of the limited number of basins and events studied, but we think the fact that the characteristic time mainly depends on the surface is a general behaviour for urbanised catchments under intense rainfall.

4. Temporal and spatial structure of rainfall

In the case of urban catchments, the typical lag time is about a few minutes to 1 h which induces a time resolution about 1–15 min for rainfall. With the HIRE'98 data set, we have the opportunity to study the temporal and spatial structure of rainfall at small scale and to investigate the impact of time averaging.

4.1. Structural analysis

Initially for mining, geostatistics (Matheron, 1965) has been developed to provide (i) a useful theoretical and mathematical description of the structural properties of natural phenomena and (ii) a practical technique to solve estimation problems. It has been also applied in water sciences (Delhomme, 1978; Creutin and Obled, 1982). In this paper, we shall use only the part of geostatistics dealing with structure identification and only a very brief overview of the needed concepts is given. For a more detailed and complete description of geostatistics, the reader can refer to Bacchi and Kottegoda (1995) or Blöschl (1999) for recent examples.

Assuming the studied spatial field is a realization of a random function Z, the structure function is given by the variogram γ:

$$\gamma(x - x') = \frac{1}{2}E\{[Z(x) - Z(x')]^2\} \tag{3}$$

The variogram is half of the expectation (E) of the quadratic increments of the random function ($[Z(x) - Z(x')]^2$), where x and x' are position vectors. The experimental variogram can be inferred from spatially distributed measurements assuming that the expectation is equal to the arithmetic mean.

In the multi-realization case (e.g. rainfall field for successive time steps), it is interesting to take into account information from all the realizations, assuming the fields to have similar statistical characteristics except for a constant factor. The variogram can therefore be normalised by the respective variance of each field considered and then averaged over all

the realizations. Assuming the structure functions have the same shape, the mean normalised variogram obtained, also called climatological variogram (Bastin et al., 1984; Lebel and Bastin, 1985), is representative of all the realizations and is less sensitive to sampling effect.

The behaviour of the variogram at the origin is described by the nugget effect: it is a possible discontinuity at the origin. Its value inferred from the experimental variogram may be due to (i) the variability at smaller scales than the sensor resolution and (ii) the measurement errors. If the random function has a defined variance, then the variogram reaches a sill at a given range. The sill corresponds to the variance (standardised to 1 for the climatological variogram) and the range to the decorrelation distance. In the following, we shall use these parameters to characterise the structure of rainfall.

In order to describe the structure by a relatively simple function (and also for the interpolation by kriging) it is necessary to fit a model to the experimental variogram. The possible function to model a variogram have to verify some mathematical properties. Among the classical model, we chose the spherical one

$$\begin{aligned} \gamma(h) &= C_0 + C\left[\frac{3}{2}\frac{d}{r} - \frac{1}{2}\left(\frac{d}{r}\right)^3\right] && \text{if } d \le r \\ \gamma(h) &= C_0 + C && \text{if } d \ge r \end{aligned} \tag{4}$$

where γ is the variogram; d, the distance; C_0, the nugget effect; C, the sill and r is the range. The three parameters we shall use to describe the structure explicitly appear in the model chosen. If the studied phenomenon results of several nested structures, a linear combination of several basic variograms can be used to model its variogram, because of the mathematical properties of the basic functions. For example, the sum of two spherical models (dual spherical model) is written

$$\begin{aligned} \gamma(d) &= C_0 + C_1\left[\frac{3}{2}\frac{d}{r_1} - \frac{1}{2}\left(\frac{d}{r_1}\right)^3\right] + C_2\left[\frac{3}{2}\frac{d}{r_2} - \frac{1}{2}\left(\frac{d}{r_2}\right)^3\right] && \text{if } d \le r_1 \\ \gamma(d) &= C_0 + C_1 + C_2\left[\frac{3}{2}\frac{d}{r_2} - \frac{1}{2}\left(\frac{d}{r_2}\right)^3\right] && \text{if } r_1 \le d \le r_2 \\ \gamma(d) &= C_0 + C_1 + C_2 && \text{if } d \ge r_2 \end{aligned} \tag{5}$$

where C_0 is the nugget effect; C_1 and r_1, the sill and the range for the first structure; C_2 and r_2, the sill and the range for the second structure.

4.2. About the temporal structure

X-VPR provides very high temporal resolution (4 s) rain measurements. We have then the opportunity to study the temporal structure of rainfall at very small scale and to study how it is affected by time integration. Time series derived from the X-VPR measurements at an altitude of 150 m (lowest altitude free of noise) have been extracted at temporal resolutions of 4 s, 1, 5 and 10 min. Although it is more usual to use a correlogram to display the decay of correlation between time steps with increasing delays, the variogram is another possible way, directly related to the correlogram.

The relief is known to influence the distribution and the amount of rainfall. Goovaerts (2000) has shown that incorporating the elevation information improves the performance of kriging methods at the monthly and annual time steps. However, because of its moderate altitude and the short time steps considered, we assume that the relief of the area has a negligible influence on the temporal and spatial structure of the studied rainfall fields.

Considering the time series of each event has the same structure function (except for a constant factor), the climatological temporal variogram over the three rain events is estimated and is displayed in Fig. 6, for the four time steps. As we think our three rain events to be representative of the Mediterranean precipitation, we assume the climatological variogram to be representative of the mean structure of Mediterranean rain events.

The variograms corresponding to the 4 s and 1 min resolutions are close and exhibit two main structures. The first one corresponds to a temporal range of about 6 min and a sill of about 0.7. It implies that

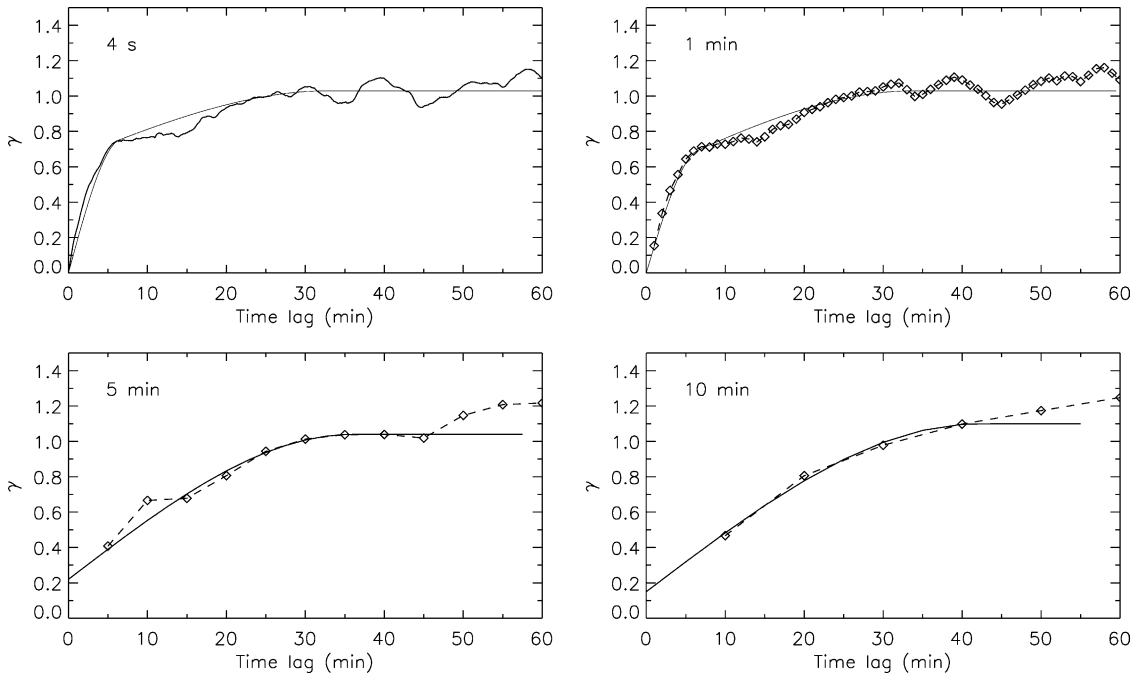

Fig. 6. Temporal climatological variograms for 4 s, 1, 5 and 10 min time resolutions, from the X-VPR measurements at an altitude of 150 m. The fitted spherical models are represented by the solid black lines.

a significant part of the temporal variability comes from this small scale structure, which may be identified as the individual convective cells. The second structure corresponds to a range of about 35 min and a sill of about 1. This longer structure may be associated to larger precipitating patterns passing over the area. We can notice the nugget effect is null for the two time resolutions, which means the temporal variability is correctly described with a 1 min time step. In order to model the variograms with two main structures, we use the dual spherical model with the sill and range associated to each structure. More complex functions could better fit the experimental variogram, but we want to use a simple one. At least, the main trend of the variograms is correctly reproduced using this dual spherical model.

When the temporal integration increases (5 and 10 min resolutions), only the larger structure remains visible on the climatological variogram. The sill is about 1 and the range is 36 min for a 5 min resolution and 42 min for a 10 min one. We can notice the nugget effect becomes positive: the time resolution is not sufficient to detect the smaller structure.

4.3. About the spatial structure

The spatial structure of rainfall is investigated using spatial climatological variograms derived from the X-RHI and the rain gauge measurements. Concerning X-RHI, we use measurements at 1 km altitude (to avoid ground echoes contamination in the vicinity of the radar) extracted from the Cartesian grids. It corresponds to 60 rain values over a horizontal distance of 15 km (resolution of 250 m). We assume the spatial structure to be similar at ground level. Concerning the rain gauges, 25 are used to estimate the spatial climatological variogram.

We follow the same approach than for the temporal structure to analyse the impact of time averaging on the spatial structure. The X-RHI measurements are averaged at 2 and 3 min and the rain gauge ones at 12 min. We can finally estimate the climatological variograms at 1, 2, 3, 6 and 12 min time resolutions.

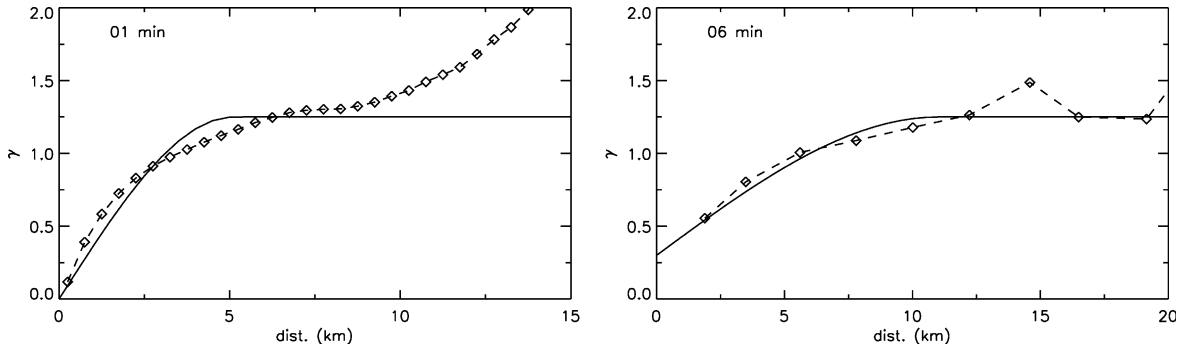

Fig. 7. Spatial climatological variogram at 1 min (from X-RHI) and 6 min (from rain gauge network) time resolutions. The fitted spherical models are represented by the solid black lines.

Longer time steps are not investigated because of the limited extents of the domains explored: 15 km for X-RHI and 15×20 km^2 for the rain gauge network. As example, the variograms at 1 and 6 min resolutions are presented in Fig. 7.

The spatial climatological variogram at 1 min time step (from X-RHI data) shows a range of 5.1 km (a nugget effect null and a sill of about 1.25). The mean horizontal advection velocity is about 13 m s^{-1}. The range value of 5.1 km is then consistent with the temporal range value of 6 min. Moreover, 5.1 km as decorrelation distance is also consistent with results obtained by Berndtsson et al. (1993) with 1 min resolution dense rain gauge network data in Sweden. It confirms that the first temporal structure corresponds to convective cells. One could expect two ranges corresponding to the two structures seen in the temporal climatological variogram. But the distance lag is limited to 15 km which is probably not enough to detect the range corresponding to the longer temporal structure.

The nugget effect for the climatological variogram at 6 min time step (from rain gauge data), about 0.3, is significantly different from 0. It shows the spatial density of rain gauges which is insufficient to detect the small scale variability at a 6 min time step.

Obtained values of range (r in km) versus time steps (Δt in min) are displayed in Fig. 8 on logarithmic axes. It can be noticed that the evolution of the range is consistent between the two different types of sensor (radar and rain gauge). The simple relation

$$r = 4.5\sqrt{\Delta t} \tag{6}$$

fits correctly the scatterplot. The same study has been conducted by Lebel et al. (1987) in a similar climatic region (Cévennes) but for 1, 2, 4, 6, 12 and 24 h time resolutions and a rain gauge density of about 1 gauge per 100 km^2. The structure observed at such space-time resolutions does not concern the convective cells but larger precipitation patterns. The values have been added in Fig. 8 together with the relation proposed by the authors ($r=25t^{0.3}$, r in km and t in h). The two scatterplots appear coherent and the two fitted relations are close, suggesting a consistency in the structure of rainfall. These relations link the spatial scale of rainfall and the temporal resolution used. However, the fitted parameters are only valid for similar climatic regions.

5. Temporal and spatial resolution for rainfall measurement

For hydrological applications, the temporal and spatial resolution of rainfall measurements depends

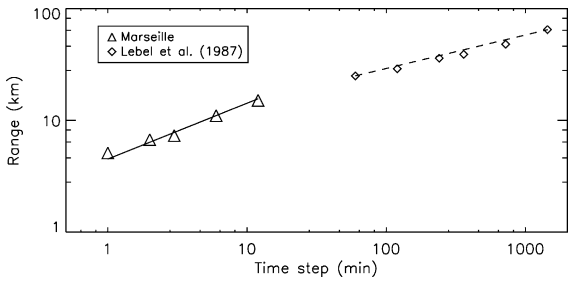

Fig. 8. Range (r in km) versus tie step (Δt in min). The black line corresponds to the relation $r=4.5\sqrt{\Delta t}$ and the dashed line to the relation $r=25\ \Delta t_h^{0.3}$ (Δt_h in h) from Lebel et al. (1987).

on the catchment to be studied. First, a catchment imposes the minimum temporal resolution necessary to correctly reproduce its dynamics. A relation between the surface of the catchment and its characteristic temporal scale has been estimated in Section 3. Therefore we have a relation between the size of the catchment (surface S in ha) and the temporal resolution required (Δt in min), based on Eqs. (1) and (2):

$$\Delta t = 0.75 S^{0.3} \tag{7}$$

Then the spatial scale of rainfall has been linked to the temporal resolution for Mediterranean climate in Section 4. Although the range is relevant to describe the spatial structure, it does not represent the domain over which a point value is representative of the average. Since the variogram increases symmetrically but rather quickly from the pivot point, a diameter of $r/3$ (where r is the range) can be retained for the spatial resolution. Journel and Huijbregts (1978) calculated the variance of the error when estimating the mean value over a square (which size is function of the range) knowing only the central point value and using a spherical model. It is of 0.13 for a size of $r/3$ which means 87% of the information is captured (this value is lower when the nugget effect is positive). Using Eq. (6), it finally leads to a relation between the temporal and the spatial resolution of rainfall measurement required for urban hydrology:

$$\Delta r = 1.5\sqrt{\Delta t} \tag{8}$$

This relation and the points corresponding to catchment surfaces of 10, 100, 1000 and 10,000 ha are plotted in Fig. 9(a). For a catchment smaller than 10 ha, the required resolution is about 1 min and 1.5 km. These values are consistent with recommendations from Schilling (1991). For a catchment of about 1000 ha, it is about 6 min and 3.7 km. For a catchment of about 10,000 ha, it is about 12 min and 5.2 km. It shows that hydrological applications require high temporal and spatial resolution for rainfall measurements. It must be noticed that because of (i) the sample of rain events we used to establish Eq. (6), the validity of Eq. (8) is restricted to similar climatic regions; and (ii) the sample of catchments we used, the validity is restricted to basins with similar geomorphological characteristics (surface between 10 and 10,000 ha, slope between 1 and 10% and imperviousness between 10 and 60%).

For a given catchment surface, the temporal resolution is directly proportional to the ratio between the temporal resolution Δt and the characteristic time t_c. It is shown in Fig. 9(b): the variations of the points corresponding to catchment surfaces of 10, 10^2, 10^3 and 10^4 ha are figured by the bold parts of the curve, when $\Delta t/t_c \in [1/5, 1/3]$. For a given catchment surface and a given ratio $\Delta t/t_c$, the spatial resolution is directly proportional to the ratio between the spatial resolution Δr and the range of the variogram r. It is shown in Fig. 9(c): the dashed lines figure the envelope of the variations of Eq. (8) when $\Delta r/r \in [1/4, 1/2]$. Because the exponent is lower than 1 in Eq. (8), the ratio $\Delta r/r$ has a more significant influence on the estimation of the spatial resolution than the ratio $\Delta t/t_c$ (for $\Delta t > 1$ min). We have chosen $\Delta r/r = 1/3$ because this value is a good compromise allowing a reliable estimation of rainfall and leading to 'reasonable' spatial resolutions. Following Schilling (1991), we have chosen $\Delta t/t_c = 1/4$. As previously explained, $\Delta t/t_c$ is a less critical parameter.

If rainfall is measured by a rain gauge network, the spatial resolution corresponds to the mean inter-distance between two gauges. A representative surface (S_r) can be associated to one rain gauge. Considering the disc which radius is half of the spatial resolution, it comes for the representative surface

$$S_r = \pi \left[\frac{\Delta r}{2}\right]^2 \tag{9}$$

on which the rainfall is relatively homogeneous at the considered time step. Then it is interesting to compare the representative surface S_r and the catchment surface S. Three cases are possible:

(1) $S_r > S$: the rainfall field is homogeneous over a surface larger than the catchment surface. A lumped modelling approach is relevant (from the rain input point of view) and the mean rain depth over the catchment can be used as input for hydrological models. Rain measurements at the catchment scale are not required because information can be deduced from outside of the catchment. For example one rain gauge close

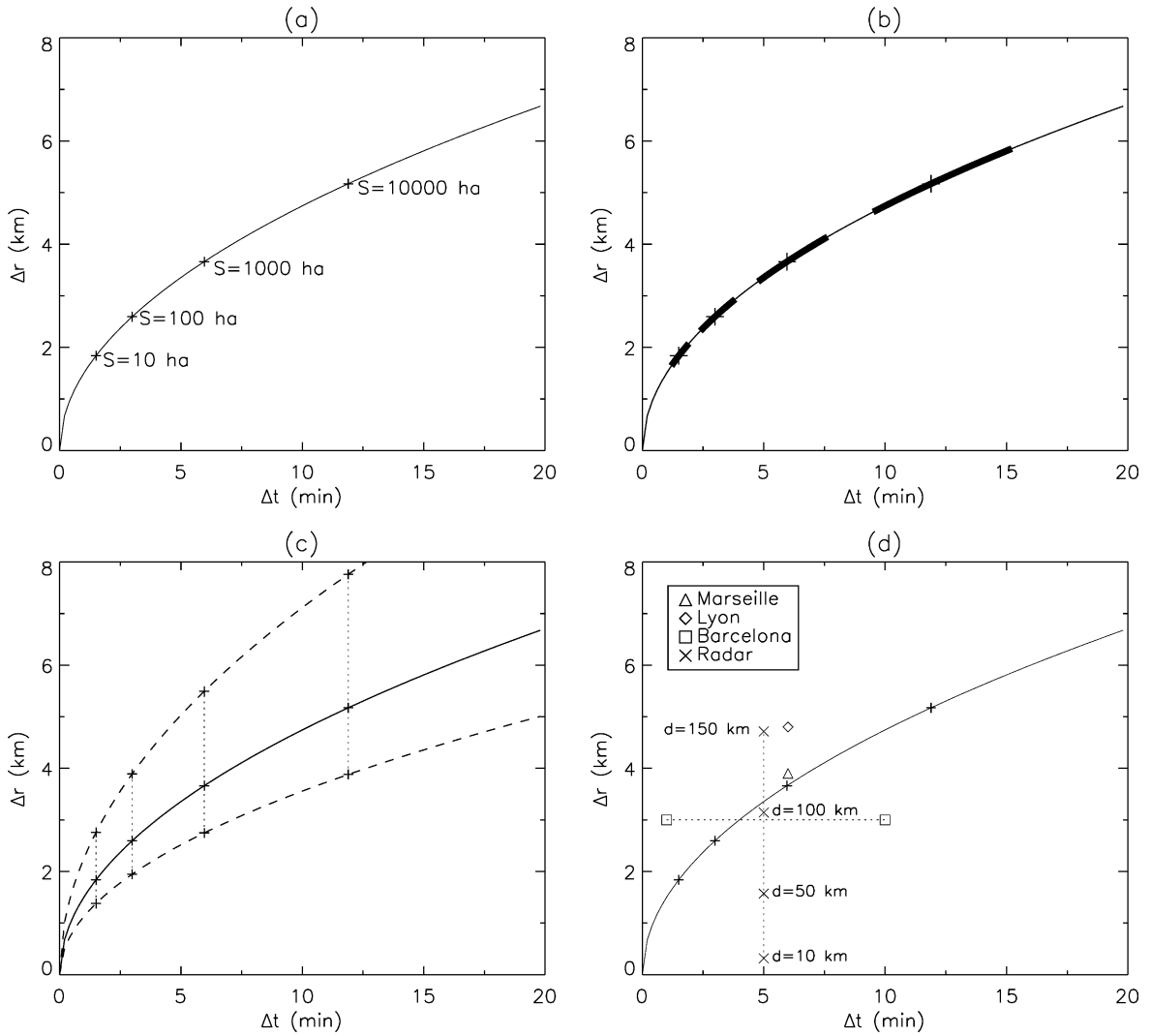

Fig. 9. (a) Spatial resolution Δr function of the temporal resolution Δt for Mediterranean rainfall. The + signs correspond to catchment surfaces of 10, 10^2, 10^3 and 10^4 ha. (b) Influence of the ratio $\Delta t/t_c$. The bold parts of the curve figure the variations of the points corresponding to the catchment surfaces when $\Delta t/t_c \in [1/5, 1/3]$. (c) Influence of the ratio $\Delta r/r$. The dashed lines figure the envelope of the variations of Eq. (8) when $\Delta r/r \in [1/4, 1/2]$. (d) The resolutions of three operational rain gauge networks and one radar are plotted. The horizontal dotted line represents the time steps available for the Barcelona network. The vertical dotted line represents the evolution of the radar spatial resolution with distance.

enough (in a way that the catchment is embedded in S_r) is sufficient.

(2) $S_r \sim S$: the rainfall field is homogeneous over a surface similar to the catchment one. A lumped modelling approach is still relevant and the mean rain depth over the entire catchment can still be used as input for hydrological applications. However, rain measurements at the catchment scale are required. For example, at least one rain gauge (with a 'central' location in the catchment) is needed.

(3) $S_r < S$: the rainfall field is homogeneous over a surface smaller than the catchment one. A lumped modelling approach is no more relevant and the rain depth must be spatially distributed. Rain measurements at a smaller scale than

the catchment one are required. For example several rain gauges must be deployed within the catchment.

Using Eq. (9), it is possible to calculate the spatial resolution corresponding to an existing rain gauge network. The network resolution appears as a point in Fig. 9(d). It is then possible to check if the network fulfils the requirements and to assess the minimum catchment size for which the data from the network can be used for hydrological purposes. To illustrate this possibility, we have represented three operational networks:

- *Marseille*: a 6 min time step and a density of about 1 gauge per 12 km^2
- *Lyon*: a 6 min time step and a density of about 1 gauge per 18 km^2
- *Barcelona*: a density of about 1 gauge per 7 km^2 and tip records. So the time step can be chosen by the user. We chose a range of time steps between 1 and 10 min for our example.

The limiting factor for hydrological applications based on data from the network of Lyon is the spatial resolution. Rain measurements can be used for hydrological applications only for catchments larger than about 6000 ha. The corresponding 'effective' time step of the rain gauge network is then about 10 min. The network of Marseille is adequate for urban catchments of about 1000 ha and the temporal and spatial resolutions are consistent. In the case of Barcelona, the possibility offered by the tip records to have very short time steps is limited to about 4 min because of the spatial resolution and hence to catchments about a few hundreds hectare. None of the operational networks presented here is adapted for the hydrology of small urban catchments (less than 100 ha).

Rainfall can also be measured using weather radar systems, which have high space-time resolutions. The temporal and the range dependent spatial resolution corresponding to an operational radar (5 min time step and 1.8° for the radar beam width) have been plotted for distances of 10, 50, 100 and 150 km. Up to 100 km, the spatial resolution is quite adapted for urban hydrology and the limiting factor is the temporal resolution, on the contrary of rain gauge networks presented. Such radar measurements can be used as input for catchments about several hundreds hectare. Beyond 100 km, the spatial resolution becomes the limiting factor. In the case of a local radar dedicated to the monitoring of an urban area, higher temporal resolutions (1 or 2 min) can be expected and then its measurements become relevant as input for hydrological modelling of very small urban catchments (about 10 ha).

Fig. 9(d) shows that urban hydrology for small catchments (surface below 100 ha) requires temporal and spatial resolution that operational networks cannot provide. The need to densify rain gauge networks and to decrease the revisiting time of weather radar systems is clearly shown. The discrepancy between the data needed for urban hydrology and the available one, already emphasised by Schilling (1991), is confirmed.

6. Conclusions

The objective of this paper was to quantify the characteristic temporal and spatial scales relevant to describe the hydrological behaviour of urbanised catchments and to estimate the minimum resolutions of rainfall required for hydrological applications over these catchments. The high resolution data set used was collected in south-east of France during the HIRE'98 experiment.

The (hydrological) characteristic time of various urban catchments has been estimated as the lag time between the mean hyetograph (the input) and the hydrograph (the output). A simple power law relation allows to link the lag time to the surface of the catchment, and so to link the temporal and the spatial scales of urbanised catchments.

Using the variogram within the geostatistics framework, the space-time structure of rainfall was studied and in particular the effect of time averaging. Again a simple relation links the spatial scale (defined as the decorrelation distance) and the time step.

Combining these relations, the minimum temporal and spatial resolution of rainfall measurements for hydrological purposes is linked to the size of the catchment. The values of resolutions obtained from quantitative investigations are in the same

order of magnitude than previously published recommendations.

The validity of the numerical relations established in this work is restricted to similar catchments (surface between 10 and 10,000 ha, slope between 1 and 10% and imperviousness between 10 and 60%) and to similar climatic regions (Mediterranean climate). However, we are convinced that the approach is relevant for various geomorphoclimatic regions.

Considering a set of urban catchments to be managed, we must notice that the space-time resolution of rainfall measurements is given by the smallest catchment. As shown in Fig. 9, the relevant resolutions for small urban catchments in Mediterranean regions require very dense rain gauge networks, which are difficult to build and to maintain, for practical and financial reasons. Weather radar offers an interesting alternative. However, one must keep in mind that its spatial resolution is range dependent and that as an indirect measurement, radar rain estimation can be affected by significant errors. Finally, the set up of rain measurement networks (based on radars or rain gauges) for urban hydrology will require important financial and human investments and supports.

Acknowledgements

The first author acknowledges financial support from the European Commission through a Marie Curie Postdoctoral Fellowship (Grant EVK1-CT-2002-50016). The authors would also like to thank Météo France, the technical services of the city of Marseille and the Water Management Research Centre (WMRC) of the University of Bristol for their collaboration during HIRE'98. The constructive comments of the three reviewers were appreciated and helped to improve the paper.

References

Bacchi, B., Kottegoda, N., 1995. Identification and calibration of spatial correlation patterns of rainfall. J. Hydrol. 165 (1–4), 311–348.

Bastin, G., Lorent, B., Duqué, C., Gevers, M., 1984. Optimal estimation of the average areal rainfall and optimal selection of rain gauge locations. Water Resour. Res. 20 (4), 463–470.

Berndtsson, R., Niemczynowicz, J., 1988. Spatial and temporal scales in rainfall analysis, some aspect and future perspectives. J. Hydrol. 100 (1–4), 293–313.

Berndtsson, R., Jinno, K., Kawamura, A., Larson, M., Niemczynowicz, J., 1993. Some Eulerian and Lagrangian statistical properties of rainfall at small space-time scales. J. Hydrol. 153 (1–4), 339–355.

Berne, A., Delrieu, G., Andrieu, H., Vignal, B. Estimating the vertical structure of intense mediterranean precipitation using two X-band weather radar systems. Submitted for publication.

Blöschl, G., 1999. Scaling issues in snow hydrology. Hydrol. Process. 13, 2149–2175.

Creutin, J.-D., Obled, C., 1982. Objective analyses and mapping techniques for rainfall fields: an objective comparison. Water Resour. Res. 18 (2), 413–431.

Delhomme, J., 1978. Kriging in the hydrosciences. Adv. Water Resour. 1 (5), 251–266.

Delrieu, G., Caoudal, S., Creutin, J.-D., 1997. Feasibility of using mountain return for the correction of ground-based X-band weather radar data. J. Atmos. Oceanic Technol. 14 (3), 368–385.

Goovaerts, P., 2000. Geostatistical approaches for incorporating elevation into the spatial interpolation of rainfall. J. Hydrol. 228 (1–2), 113–129.

Journel, A., Huijbregts, C., 1978. Mining Geostatistics. Academic Press, London.

Lebel, T., Bastin, G., 1985. Variogram identification by the mean-square interpolation error method with application to hydrologic fields. J. Hydrol. 77 (1–4), 31–56.

Lebel, T., Bastin, G., Obled, C., Creutin, J.-D., 1987. On the accuracy of areal rainfall estimation: a case study. Water Resour. Res. 23 (11), 2123–2134.

Matheron, G., 1965. Les Variables Régionalisées et Leur Estimation. Masson et Cie, Paris.

Morin, E., Enzel, Y., Shamir, U., Garti, R., 2001. The characteristic time scale for basin hydrological response using radar data. J. Hydrol. 252 (1–4), 85–99.

Niemczynowic, J., 1999. Urban hydrology and water management—present and future challenges. Urban Water 1 (1), 1–14.

Ogden, F., Sharif, H., Senarath, S., Smith, J., Baeck, M., Richardson, J., 2000. Hydrologic analysis of the Fort Collins, Colorado, flash floods of 1997. J. Hydrol. 228 (1–2), 82–100.

Schaake, J., Geyer, J., Knapp, J., 1967. Experimental examination of the rational method. J. Hydr. Div., Proc. ASCE HY6, 353–370.

Schilling, W., 1991. Rainfall data for urban hydrology: what do we need? Atmos. Res. 27 (1–3), 5–21.

Uijlenhoet, R., Andrieu, H., Austin, G., Baltas, E., Borga, M., Brilly, M., Cluckie, I., Creutin, J.-D., Delrieu, G., Deshons, P., Fatorelli, S., Griffith, R.P.G., Hang, D., Mimikou, M., Moani, M., Porrà, J., Sempere-Torres, D., Spangi, D., 1999. Hydromet integrated radar experiment (HIRE): experimental setup and first results, in: 29th Conference on Radar Meteorology. AMS, Montréal, Canada, pp. 926–930.